The interplay of multiple feedback loops with post-translational kinetics results in bistability of mycobacterial stress response

Abhinav Tiwari[1], **Gábor Balázsi**[2], **Maria Laura Gennaro**[3] **and Oleg A Igoshin**[1]

[1] Department of Bioengineering, Rice University, MS-142, 6100 Main St., Houston, TX 77005, USA
[2] Department of Systems Biology—Unit 950, The University of Texas MD Anderson Cancer Center, Houston, TX 77054, USA
[3] Public Health Research Institute, New Jersey Medical School, 225 Warren Street, Newark, NJ 07103, USA

E-mail: igoshin@rice.edu

Abstract

Bacterial persistence is the phenomenon in which a genetically identical fraction of a bacterial population can survive exposure to stress by reduction or cessation of growth. Persistence in mycobacteria has been recently linked to a stress-response network, consisting of the MprA/MprB two-component system and alternative sigma factor σ^E. This network contains multiple positive transcriptional feedback loops which may give rise to bistability, making it a good candidate for controlling the mycobacterial persistence switch. To analyze the possibility of bistability, we develop a method that involves decoupling of the network into transcriptional and post-translational interaction modules. As a result we reduce the dimensionality of the dynamical system and independently analyze input–output relations in the two modules to formulate a necessary condition for bistability in terms of their logarithmic gains. We show that neither the positive autoregulation in the MprA/MprB network nor the σ^E-mediated transcriptional feedback is sufficient to induce bistability in a biochemically realistic parameter range. Nonetheless, inclusion of the post-translational regulation of σ^E by RseA increases the effective cooperativity of the system, resulting in bistability that is robust to parameter variation. We predict that overexpression or deletion of RseA, the key element controlling the ultrasensitive response, can eliminate bistability.

S Online supplementary data available from stacks.iop.org/PhysBio/7/036005/mmedia

(Some figures in this article are in colour only in the electronic version)

1. Introduction

Persistence is a distinct physiological state in which a genetically identical fraction of a bacterial population can survive exposure to stress such as antibiotics and thereafter grow to regenerate a population with the same antibiotic sensitivity [1]. This effect has been linked to the inherent phenotypic heterogeneity in microbial populations [2]; persister cells in *Escherichia coli* have been shown to display either reduced growth rates or a non-growing phenotype [3, 4]. In the pathogen *Mycobacterium tuberculosis*, persistence is one of the primary forces in successful colonization of the host,
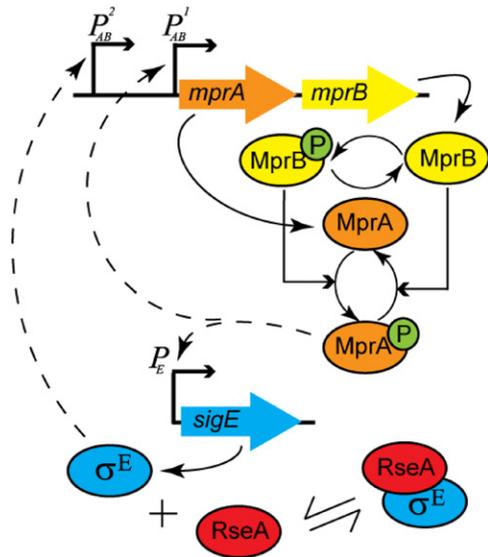
Figure 1. Schematic of the stress-response network in mycobacteria, depicting transcriptional and post-translational interactions. Dashed lines represent transcriptional regulation. The phosphorylation state of MprA is modulated through the phosphorylation–dephosphorylation reactions controlled by MprB. Phosphorylated MprA (MprA~P) upregulates transcription of the *mprAB* and *sigE* operons. The activity of σ^E is regulated by binding of the anti-sigma factor RseA. Only free σ^E upregulates transcription of the *mprAB* operon.

because persistent bacteria avoid elimination by the immune response or by drugs [5]. With no or very slow replication, these pathogens can persist in a latent state for years [6]. Although multiple genes associated with persistence in *M. tuberculosis* have been identified [7–9], the detailed molecular mechanisms underlying the phenotypic switch to persistence remain unknown.

Mycobacterial persistence has been associated recently with the stress-response network, schematically depicted in figure 1, containing the MprA/MprB two-component system (TCS) along with the alternative sigma factor σ^E and its anti-sigma factor RseA. MprA, the transcriptional regulator of the TCS, has been reported to be essential for mycobacterial persistence [8]. Moreover, upregulation of σ^E expression has been observed in various stress conditions such as nutrient depletion, heat shock and exposure to oxidizing agents and detergents [10–12], all of which mimic persistence-inducing environmental changes. Importantly, σ^E mediates transcription of the stringent response regulator *relA,* which regulates the expression of antigenic and enzymatic factors required for mycobacterial persistence [13]. The network is triggered by autophosphorylation of MprB [14], the sensor histidine kinase of the TCS, in the presence of polyphosphate as a phosphate donor [15]. The phosphate is then transferred to MprA, thereby activating it [14]. MprB is a bifunctional enzyme also capable of dephosphorylating phosphorylated MprA (MprA~P) [14]. σ^E activity is post-translationally regulated by the anti-sigma factor RseA [16], which binds to σ^E in reducing environments [17]. Positive autoregulation of the *mprAB* operon due to transcriptional regulation by

MprA~P gives rises to a positive feedback loop [18]. The second feedback loop arises from transcriptional activation of *sigE* by MprA~P [19] and subsequent upregulation of *mprAB* transcription from an σ^E-dependent promoter [11].

A study of *relA* transcription dynamics from an σ^E-dependent promoter in single *Mycobacterium smegmatis* cells revealed bimodal distribution of gene expression in the population [20]. This bimodality was hypothesized to be associated with bistability in the upstream MprA/MprB network originating from its transcriptional autoregulation. The accompanying mathematical model indeed suggested that bistability is possible under certain parameter values and biochemical assumptions, including the phosphatase activity of the phosphorylated form of MprB (MprB~P), which dephosphorylates MprA~P. Experimental results suggest, however, that nonphosphorylated MprB acts as a phosphatase in the above reaction [14], as it does in many other bacterial TCSs [21]. Recently, a stochastic kinetic model of TCSs with the correct dephosphorylation mechanism was constructed [22]. This model showed that TCSs can exhibit all-or-none, graded or mixed-mode responses depending on the actual kinetic parameters. However, this model did not include a feedback for the sensor histidine kinase from phosphorylated response regulator similar to what occurs in DegS/DegU TCS in *Bacillus subtilis* [23]. Moreover, for the MprA/MprB TCS both *mprA* and *mprB* genes are cotranscribed from one autoregulated operon, making the model of [22] inapplicable. Thus, we re-examine here the mechanism of the bistability in the network controlling *relA* expression, including both the phosphatase activity and the positive feedback associated with MprB.

We hypothesize that the multiple positive feedback loops in the network architecture may lead to bistable behavior of this circuit (one state corresponding to basal expression of *mprAB* and *sigE* and the other to near maximal expression), thereby making it a good candidate for the persistence switch. To test this hypothesis, we construct a comprehensive mathematical model and develop a novel approach to analyze this stress-response network for the presence of bistability. We examine the dynamics of various reduced versions of the full network to understand the role of each component in generating bistability. We first analyze the autoregulated MprA/MprB TCS studied in [20] and find that the TCS is not bistable in a biochemically relevant parameter range. We then introduce the second positive feedback loop via the transcriptional regulation of the *sigE* operon by MprA~P and of the *mprAB* operon by an σ^E-dependent promoter. We find that the second positive feedback loop is insufficient to induce bistability because it weakens the overall positive feedback. Finally, we include the post-translational regulation of σ^E by the anti-sigma factor RseA. This interaction significantly increases the effective cooperativity and leads the system to bistability, which is robust to parameter variation. Thus, by investigating the role of multiple feedback loops in the network architecture we decipher the mechanisms controlling bistability in the mycobacterial stress-response network.

2. Results

2.1. Necessary condition for bistability

The presence of a positive feedback in a biochemical network has been shown to be a necessary, but not sufficient, condition for system to be bistable [24, 25]. Here, we develop a new approach to establish a stricter necessary condition for bistability. Moreover, we show that such a condition can sometimes be sufficient to find a region of bistability, given the freedom to adjust certain biochemical parameters characterizing feedback interactions. We sketch the general ideas of the approach in this section and show the detailed steps of the treatment in the Methods section.

Generally, the dynamical systems' representation of biochemical networks comprises more than three ordinary-differential equations, making graphical or analytical stability analysis impossible. However, since protein translation and transcription reactions are often slower than the post-translational steps [26], a system can be decoupled into two modules: a *post-translational interaction module* describing system dynamics at the quasi-steady state by algebraic equations and a *transcriptional regulation module* describing dynamics of the total concentrations of each chemical species (conserved in the post-translational module) with ordinary differential equations. This separation greatly reduces the dimensionality of the dynamical systems and thereby enables independent input–output analysis in the two modules.

The transcriptional regulation module relates the rate of change of the total protein concentration vector ($\mathbf{X_T} = \left[X_T^1, X_T^2, \ldots, X_T^N\right]$) to the concentration vector of the active forms of transcription factors ($\mathbf{X_A} = \left[X_A^1, X_A^2, \ldots, X_A^M\right]$):

$$\frac{\mathrm{d}\mathbf{X_T}}{\mathrm{d}t} = k_{\mathrm{pdeg}} \left\{ \mathbf{F}\left(\left[X_A^1, X_A^2, \ldots, X_A^M\right]\right) - \mathbf{X_T} \right\}$$
$$= k_{\mathrm{pdeg}} \left\{ \mathbf{F}(\mathbf{X_A}) - \mathbf{X_T} \right\},$$

where $\mathbf{F}(\mathbf{X_A}) = [F_1(\mathbf{X_A}), F_2(\mathbf{X_A}), \ldots, F_N(\mathbf{X_A})]$ is the vector of protein production normalized by the k_{pdeg} protein degradation rate constant, assumed to be same for all protein forms for notation simplicity. The components of the concentration vectors X_T^i ($i = 1, \ldots, N$) and X_A^i ($i = 1, \ldots, M \leqslant N$) correspond to the concentrations of the total protein and the active forms of the transcription factors, respectively. In the post-translational interaction module in the absence of protein production or degradation, considering that these processes are relatively slow, we analyze the steady-state levels of active forms of the transcription factors, represented by the vector $\mathbf{X_A}$ as functions of total protein concentrations $\mathbf{X_T}$ in the absence of protein production or degradation:

$$\mathbf{X_A} = \mathbf{G}\left(\left[X_T^1, X_T^2, \ldots, X_T^N\right]\right) = \mathbf{G}(\mathbf{X_T}).$$

Thus, the input to one module is the output from the other and vice versa, and at the steady state $\mathbf{X_T} = \mathbf{F}(\mathbf{X_A}) = \mathbf{F}(\mathbf{G}(\mathbf{X_T}))$. The stability of the system is determined by the Jacobian matrix $J_{ij} = \partial F_i(\mathbf{G}(\mathbf{X_T})) / \partial X_T^j$.

In a one-dimensional dynamical system, graphical analysis is useful as steady states correspond to intersections of curves $X_T = F(X_A)$ and $X_A = G(X_T)$, and their stability is denoted by their respective slopes. These slopes can be

easily expressed in terms of the logarithmic gains (LGs) of the modules LG_T (transcriptional) and LG_P (post-translational), which are effective kinetic orders of the power-law system representation [27]. To obtain multistability, at least one unstable steady state must exist, which requires that the inequality $\mathrm{LG}_T^{-1} < \mathrm{LG}_P$ be satisfied. As a result of decoupling approximation, the LGs of the two modules depend on non-overlapping sets of biochemical parameters, thereby simplifying the analysis and search for bistability. The post-translational interaction module contains only the post-translational rate constants, while the transcriptional regulation module involves protein synthesis and degradation rates. Therefore, the search for bistability is effectively transformed into two independent optimization problems of maximizing the LGs.

2.2. Bistability in the MprA/MprB TCS

A recent work showed bimodal distribution of *relA* expression in the population which was hypothesized to originate from the positive feedback due to transcriptional autoregulation in the MprA/MprB TCS [20]. These results were explained by an accompanying mathematical model which included the assumption that the phosphorylated form of MprB (MprB∼P) functions as a phosphatase for dephosphorylating MprA∼P. Experimental results suggest, however, that the unphosphorylated form of MprB functions as a phosphatase in that reaction [14]. Thus, the bistable behavior must be re-examined within a framework that incorporates the experimentally observed molecular interactions. Below we analyze the reduced network comprising the MprA/MprB TCS (figure 2(*a*)) and show that biochemically realistic parameters in this network do not result in bistability.

To illustrate the derivation of the necessary condition involving the LGs, we analyze the MprA/MprB TCS (figure 2(*a*)). Using the decoupling approximation described above and in [28], we divide the MprA/MprB TCS into an autoregulation module and a phosphorylation module, which respectively comprise transcriptional regulation and quasi-steady state approximation of post-translational interactions present in the system. The various interactions are modeled as a set of ordinary differential equations which, after simplifications (see section 4), can be described by two dynamical equations, one for total MprA (A_T) concentration and another for phosphorylated MprA (A_P) concentration, which are the input–output signals of the two modules:

$$\frac{\mathrm{d}A_T}{\mathrm{d}t} = k_{\mathrm{pdeg}} \left[F(A_P) - A_T\right] \tag{1}$$

$$A_P = G(A_T), \tag{2}$$

where F and G represent the functional dependence of A_T and A_P on each other in the autoregulation and the phosphorylation modules, respectively (cf equations (35), (28)–(31)), while k_{pdeg} is the protein degradation rate.

In a one-dimensional dynamical system, the existence of two stable steady states requires the existence of an unstable steady state in between. Linearizing (1) and (2) around the steady state $\left(A_T^0, A_P^0\right)$ and using the definition of LGs of the
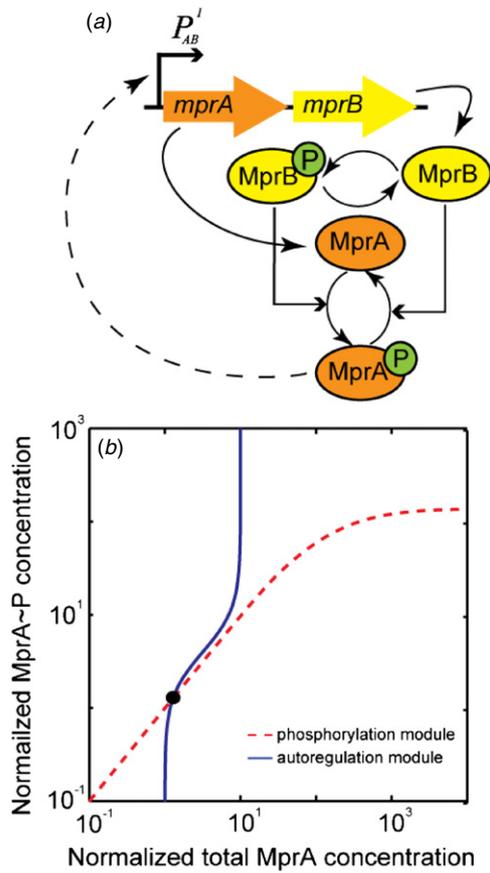
Figure 2. Bistability in the MprA/MprB TCS. (*a*) Reduced network consisting only of the MprA/MprB TCS. (*b*) The steady-state circuit output (A_P) is controlled by the intersection of the phosphorylation and autoregulation curves describing the relationship between total (A_T) and phosphorylated MprA (A_P) concentrations (see section 4 for details). In the physiologically relevant range of the amplification gain ($f_1 = 10$) and in the absence of an external phosphatase dominating the dephosphorylation flux of MprA$\sim$P ($k_{\text{exd}} = 0$), the MprA/MprB TCS is not bistable regardless of other parameters. The only stable steady state is represented by the filled circle at the intersection of the two curves.

autoregulation and phosphorylation modules at the steady state $\left(F\left(A_P^0\right) = A_T^0, G\left(A_T^0\right) = A_P^0 \right)$,

$$\text{LG}_A = \left. \frac{A_P^0}{F} \frac{\partial F}{\partial A_P} \right|_{A_P = A_P^0} \quad \text{and} \quad \text{LG}_P = \left. \frac{A_T^0}{G} \frac{\partial G}{\partial A_T} \right|_{A_T = A_T^0} \tag{3}$$

we obtain the following equation for perturbation $\varepsilon_1(t)$ in A_T:

$$\frac{\mathrm{d}\varepsilon_1}{\mathrm{d}t} = k_{\text{pdeg}} \left(\text{LG}_A \text{LG}_P - 1 \right) \varepsilon_1. \tag{4}$$

Inspecting (4), we conclude that, for at least one unstable steady state and bistability to exist, the product LG_ALG_P must be greater than 1. Thus, we arrive at the following necessary condition for bistability:

$$\frac{1}{\text{LG}_A} < \text{LG}_P. \tag{5}$$

This condition is used later to examine the presence of bistability in various subnetworks and ultimately in the mycobacterial stress-response network.

Using the decoupling approximation (equations (1) and (2)), we examine the network as a combination of autoregulation and phosphorylation modules. We use (5), the necessary condition based on LGs, to explore bistability in the MprA/MprB TCS at the steady state. The LG for the autoregulation module (3) was calculated analytically using (1) at the steady state, with F defined in (35):

$$\text{LG}_A = \frac{2 \frac{A_P^2}{K_1} (f_1 - 1)}{\left(1 + \frac{A_P^2}{K_1}\right)\left(1 + f_1 \frac{A_P^2}{K_1}\right)}, \tag{6}$$

where f_1 is the amplification gain and K_1 is the equilibrium constant for dissociation of two MprA$\sim$P molecules from DNA (the transcriptionally active form of MprA is the phosphorylated dimer [18]). The equations for the phosphorylation module are not analytically tractable and therefore we compute the LG either numerically or analytically under certain approximations.

Since LG_A and LG_P depend on non-overlapping sets of parameters, we reduce checking for bistability to two independent optimization problems of maximizing the LGs. Using (6), we analytically compute the maximum value of LG_A over the range of A_P:

$$\max(\text{LG}_A) = 2 \frac{(\sqrt{f_1} - 1)}{(\sqrt{f_1} + 1)}. \tag{7}$$

This expression depends only on the amplification gain f_1: $\max(\text{LG}_A)$ increases with f_1 such that for $f_1 = 9$ it is 1, while for $f_1 \to \infty$ it is 2.

We numerically compute the maximum value of LG_P, which is found to depend on the predominant biochemical mechanism of MprA$\sim$P dephosphorylation. If the dephosphorylation is dominated by MprB (which is expected since MprB is a bifunctional enzyme and no external phosphatase has been identified in this system), then $\max(\text{LG}_P)$ is 1. This result can be analytically demonstrated for the reduced model with no exogeneous phosphorylation–dephosphorylation of MprA and irreversible autophosphorylation of MprB (cf equation (36)). This limit was also considered in [21, 29].

Therefore, the left-hand side of (5) for the MprA/MprB system is greater than 1. In contrast, the right-hand side is smaller than 1 in the absence of exogenous phosphatase activity. Together these results indicate that the MprA/MprB TCS does not satisfy the necessary condition (5) for measured amplification gain ($f_1 \approx 8$) [19, 30] (figure 2(*b*)). The only stable steady state is represented by the filled circle on the intersection of autoregulation and phosphorylation curves. Nonetheless, we can obtain bistability in an autoregulated TCS under certain conditions not applicable to the MprA/MprB system (supplementary figure S1 available at stacks.iop.org/PhysBio/7/036005/mmedia).

It should be noted that the value for amplification gain used in the above analysis has been estimated from experimental data on *M. tuberculosis* (supplementary information available at stacks.iop.org/PhysBio/7/036005/mmedia). We hypothesize that these estimates can be used in our model of bistability in *M. smegmatis* because MprA/MprB TCS and σ^{E} are highly conserved in mycobacteria [8, 31].

2.3. Indirect σ^E-mediated feedback does not make the TCS bistable

In the absence of the anti-sigma factor RseA, free σ^E upregulates transcription of the *mprAB* operon [11]. In addition, the *sigE* operon is upregulated by the TCS transcriptional regulator, MprA∼P [19]. The net effect of these transcriptional regulations can be perceived as a σ^E-mediated indirect feedback to the *mprAB* operon. Therefore, it is possible that this indirect feedback in combination with the direct feedback analyzed in the preceding subsection can lead to bistability in the network. For simplicity, we first analyze the network in the absence of post-translational regulation of σ^E by RseA (figure 3(*a*)).

We model the distinct σ^E-dependent and MprA∼P-regulated promoters of the *mprAB* operon by considering their effects in an additive fashion such that the total transcription is the sum of the individual transcriptional rates. Application of decoupling approximation to this network leads to the following two-dimensional system for the total concentrations of MprA (A_T) and σ^E (E_T):

$$\frac{\mathrm{d}A_T}{\mathrm{d}t} = k_{\mathrm{pdeg}}[F^D(A_P) + F^I(E_T) - A_T] \qquad (8)$$

$$\frac{\mathrm{d}E_T}{\mathrm{d}t} = k_{\mathrm{pdeg}}[H(A_P) - E_T], \qquad (9)$$

where F^D and F^I represent transcription of the *mprAB* operon due to direct and σ^E-mediated indirect feedbacks, respectively; $H(A_P)$ represents transcription of the *sigE* operon due to MprA∼P regulation and k_{pdeg} is the protein degradation rate (cf equation (37)). These equations along with (2) describe the MprA/MprB/σ^E network dynamics and can be further reduced to a one-dimensional system by following the nullcline $E_T = H(A_P)$. Biochemically, this corresponds to a quasi-steady state approximation for E_T and analyzing the effect of the additional feedback through its contribution to the LG of the autoregulation module. This reduced system is described by equations (1) and (2) with

$$F(A_P) = F^D(A_P) + F^I(H(A_P)). \qquad (10)$$

We use the necessary condition described earlier to analyze this one-dimensional system for bistability. The necessary condition for bistability in the two-dimensional system is also calculated and found to be identical to that of the one-dimensional system (supplementary information available at stacks.iop.org/PhysBio/7/036005/mmedia). This equivalence justifies our quasi-steady state approximation for E_T.

Generally, the LG of the sum of two fluxes is given by a weighted average of the LGs of individual fluxes with weights being their fractional contribution to the total flux:

$$\mathrm{LG}(y_1 + y_2) = \frac{y_1}{y_1 + y_2}\mathrm{LG}(y_1) + \frac{y_2}{y_1 + y_2}\mathrm{LG}(y_2). \qquad (11)$$

Thus, the net LG due to combination of the direct and indirect feedbacks is given by the following expression:

$$\mathrm{LG}_A^T = \omega \mathrm{LG}_A^D + (1 - \omega)\,\mathrm{LG}_A^I, \qquad (12)$$

where ω is the fraction of transcription that takes place via the direct feedback loop, and $\mathrm{LG}_A^D = \frac{A_P}{F^D}\frac{\partial F^D}{\partial A_P}$ and $\mathrm{LG}_A^I = \frac{A_P}{F^I}\frac{\partial F^I}{\partial A_P}$
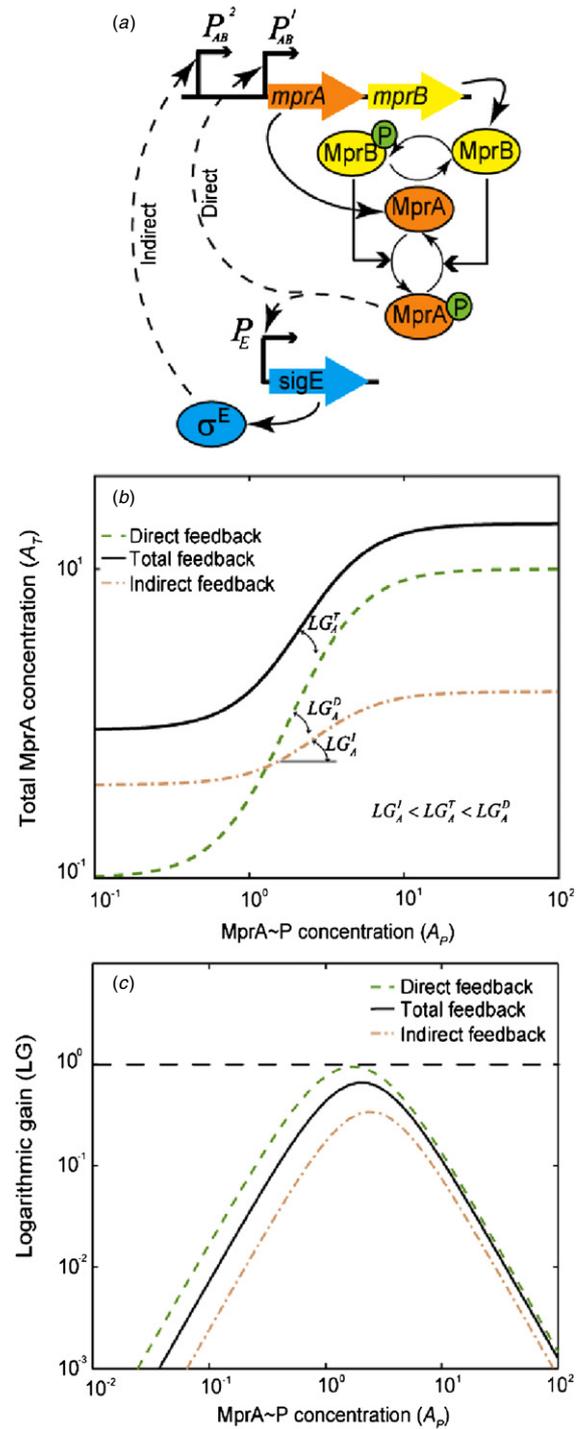
Figure 3. Without the anti-sigma factor, the σ^E-mediated feedback decreases the logarithmic gain (LG) of the autoregulation module. (*a*) The reduced network consisting of the MprA/MprB TCS and sigma factor σ^E, but no anti-sigma factor RseA. (*b*) Autoregulation curves for the cases with direct, indirect and total feedbacks. LG_A^D and LG_A^I are the autoregulation module LGs for the direct feedback due to autoregulation in the TCS and the indirect feedback due to the transcriptional regulation of the *mprAB* operon by σ^E. LG_A^T is the total LG for the autoregulation module in the reduced network. Inclusion of an additional feedback due to σ^E decreases the total LG ($\mathrm{LG}_A^T < \mathrm{LG}_A^D$), thereby preventing the necessary condition for bistability to be satisfied. (*c*) LG curves for the cases with direct, indirect and total feedbacks. The dotted line (LG = 1) represents the maximum LG for the phosphorylation module.

are the LGs of the autoregulation module due to the direct feedback (equation (6)) and the indirect feedback, respectively. The expression for LG_A^I is the same as LG_A^D, with f_1 and K_1 replaced by f_{eff} and K_{eff}, respectively. f_{eff} is the effective amplification gain due to the indirect feedback composed of the transcriptional regulation of the *sigE* operon by MprA~P and of the *mprAB* operon by σ^{E}, and K_{eff} is the effective dissociation constant for MprA~P–DNA binding in the case of the indirect feedback. Maximum LG_A^I can be represented by an expression similar to that for LG_A^D (equation (7)):

$$\max\left(\mathrm{LG}_A^I\right) = 2\frac{(\sqrt{f_{\mathrm{eff}}} - 1)}{(\sqrt{f_{\mathrm{eff}}} + 1)}. \tag{13}$$

This maximum occurs at the maximal value of f_{eff} (cf equation (41)) which is a function of f_2 and f_3, the amplification gains for the transcriptional regulation of the *mprAB* and *sigE* operons by σ^{E} and MprA~P, respectively. Using equation (41), it can be shown that $\max(f_{\mathrm{eff}}) < f_2$ and $\max(f_{\mathrm{eff}}) < f_3$. Moreover, since f_1, f_2 and f_3 are of the same order [11, 19, 30],

$$\max(f_{\mathrm{eff}}) < f_1. \tag{14}$$

From (7), (13) and (14), we obtain

$$\max\left(\mathrm{LG}_A^I\right) < \max\left(\mathrm{LG}_A^D\right). \tag{15}$$

Based on (12), the weighted average of the two LGs will be smaller than the maximum. Thus, introduction of the indirect feedback via σ^{E} into the network makes bistability less likely because the σ^{E}-mediated feedback decreases the LG of the autoregulation module in the MprA/MprB/σ^{E} network. This result is depicted in figures 3(*b*) and (*c*), where panel (*b*) shows input–output curves for the autoregulation module in the cases of the direct feedback, indirect feedback and total feedback, in which the slopes of curves represent the LGs. Figure 3(*c*) illustrates our analytical result: $\mathrm{LG}_A^I < \mathrm{LG}_A^T < \mathrm{LG}_A^D$. Conclusively, the decrease in LG_A prevents the necessary condition for bistability to be satisfied and hence an additional feedback through σ^{E} does not make the system bistable.

2.4. Autoregulated σ^{E}–RseA network is bistable

In mycobacteria, σ^{E} activity is regulated by the anti-sigma factor RseA which is encoded in the operon downstream of *sigE* [32]. To incorporate this post-translational regulation of σ^{E} we study the reduced network comprising the σ^{E}–RseA interaction and positive autoregulation of the *sigE* operon (figure 4(*a*)). The positive autoregulation is a result of either indirect feedback via the MprA/MprB TCS [11, 30] or the putative direct autoregulation effect of σ^{E} on its own transcription [11]. In this subsection, we phenomenologically model the autoregulation with the Hill equation (cf equation (42)) to allow closed-form analytical results. We analyze this reduced network by decomposing it into σ^{E} autoregulation and σ^{E}–RseA interaction modules, described by the following equations:

$$\frac{\mathrm{d}E_T}{\mathrm{d}t} = k_{\mathrm{pdeg}}\left[U(E) - E_T\right] \tag{16}$$

$$E = V(E_T), \tag{17}$$

where U and V represent the functional dependence of total σ^{E} (E_T) and free σ^{E} (E) concentrations on each other in the autoregulation and the interaction module, respectively (cf equations (42) and (32)), while k_{pdeg} is the protein degradation rate.

This separation allows us to analytically calculate the LGs for the autoregulation $\left(\mathrm{LG}_A = \frac{E}{U}\frac{\partial U}{\partial E}\right)$ and interaction modules $\left(\mathrm{LG}_I = \frac{E_T}{V}\frac{\partial V}{\partial E_T}\right)$ (cf equations (43) and (44)). Using these we analytically compute expressions for the maximum values of these LGs:

$$\max(\mathrm{LG}_A) = q\frac{(\sqrt{f} - 1)}{(\sqrt{f} + 1)} \tag{18}$$

$$\max(\mathrm{LG}_I) = \frac{\left(2\sqrt{\frac{K_D}{R_T}\left(\frac{K_D}{R_T} + 1\right)} + 1 + 2\frac{K_D}{R_T}\right)}{2\left(\sqrt{\frac{K_D}{R_T}\left(\frac{K_D}{R_T} + 1\right)} + \frac{K_D}{R_T}\right)}, \tag{19}$$

where f is the amplification gain due to positive autoregulation by σ^{E}; q is the Hill coefficient representing effective cooperativity in the autoregulation module; R_T is the total RseA concentration and K_D is the dissociation constant for the σ^{E}–RseA interaction complex.

From (19) we conclude that $\max(\mathrm{LG}_I)$ increases with decreased K_D, i.e. with increased σ^{E}–RseA interaction strength (figure 4(*b*)). By analyzing (18) and (19) we conclude that, given a sufficiently strong σ^{E}–RseA interaction, we can find parameters to satisfy the necessary condition:

$$\frac{1}{\max(\mathrm{LG}_A)} < \max(\mathrm{LG}_I). \tag{20}$$

Thus, regardless of the amplification gain and the effective cooperativity in the autoregulation module, we can find a parameter set such that the σ^{E}–RseA network is bistable. Figure 4(*c*) demonstrates bistability in the autoregulated σ^{E}–RseA network for a sample parameter set. The two filled circles on intersections of the autoregulation and interaction curves represent the stable steady states, whereas the empty circle between is the unstable steady state. In conclusion, we show that the σ^{E}–RseA interaction can significantly increase effective cooperativity and thereby lead to bistability in the presence of positive autoregulation. The increase in effective cooperativity leading to an ultrasensitive response is characteristic of systems where protein is sequestered by an inhibitor [33–35].

2.5. Bistability in the complete mycobacterial stress-response network

The promising result in the previous section paved the way for analysis of the integrated mycobacterial stress-response network comprising the MprA/MprB TCS and the σ^{E}–RseA circuit. We study the complete network by decoupling it into autoregulation and interaction modules. Also, we replace the phenomenological (Hill equation) model of σ^{E} autoregulation with a more rigorous mathematical model explicitly incorporating the transcriptional regulation of the *mprAB* and *sigE* operons by σ^{E} and MprA~P, respectively (cf supplementary equations
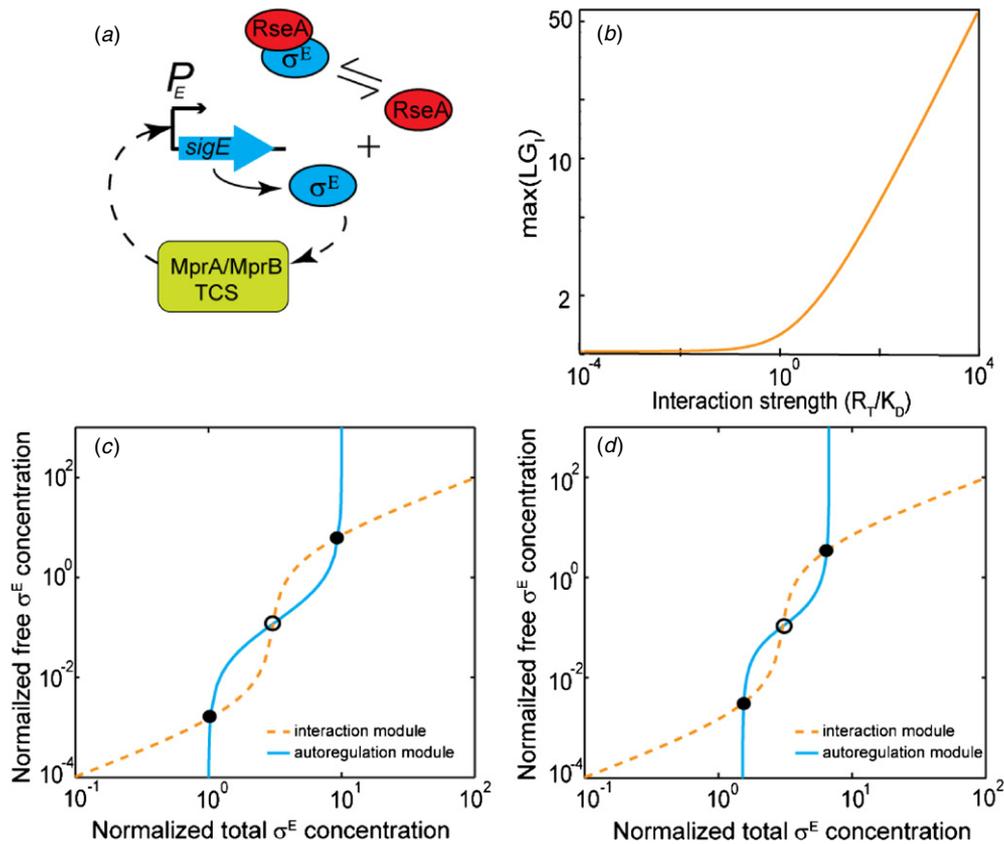
Figure 4. Interaction between σ/anti-σ leads to bistability in the mycobacterial stress-response network. (*a*) The reduced network consisting of the σ^E/RseA interaction and the positive autoregulation (dashed lines) by σ^E. (*b*) The maximum value of the logarithmic gain of the interaction module (LG$_I$) increases with σ/anti-σ interaction strength (low K_D). (*c*), (*d*) The steady-state circuit output (*E*) in the reduced network and in the complete network consisting of the MprA/MprB TCS and the σ^E–RseA circuit is controlled by intersection of the interaction and the autoregulation curves describing the relationship between the total (E_T) and the free σ^E (*E*) concentrations. Both the σ^E–RseA reduced network (*c*) and the complete network (*d*) are bistable; the two filled circles represent the stable steady states, while the empty circle between is the unstable steady state.

(S39)–(S43) mentioned here and elsewhere in the text are available at stacks.iop.org/PhysBio/7/036005/mmedia). Therefore, the autoregulation curve for the complete network changes in comparison to that for the σ^E–RseA reduced network, whereas the interaction curve remains the same (cf figures 4(*c*) and (*d*)). We conclude that the complete network is bistable for a sample parameter set. The two filled circles on intersections of the autoregulation and interaction curves represent the stable steady states, while the empty circle in between is the unstable steady state (figure 4(*d*)). Thus, the mycobacterial stress-response network is bistable in a biochemically feasible range of parameters.

We performed full network bifurcation analysis to understand bistability in greater detail and to study its dependence on physiologically relevant network parameters. The mycobacterial stress-response pathway is triggered by polyphosphate kinase activity [15], which catalyzes the synthesis of polyphosphate. Polyphosphate, a linear polymer of orthophosphate residues, serves as a phosphate donor in the MprB autophosphorylation reaction. Eventually, the phosphorylation state of MprB modulates MprA activity through phosphorylation–dephosphorylation reactions. Therefore, MprB autophosphorylation rate (k_{ap}) is an important physiological input to the system. Also,

MprA~P and free σ^E concentrations are good measures of system output as they are the transcriptional regulators controlling the expression of numerous downstream genes involved in stress response. Thus, in figures 5(*a*) and (*b*) we plot the steady-state MprA~P (A_P) and free σ^E (*E*) concentrations, respectively, as a function of MprB autophosphorylation rate (k_{ap}). In each figure, the two solid lines represent the stable steady states, which are separated by the unstable steady state (dotted line). The system displays a bistable response, which indicates the existence of two stable steady states for an intermediate range of autophosphorylation rates. The system can reach either of the two steady states depending on the initial conditions.

To evaluate the general applicability of our conclusions to biological situations, we analyze the robustness of bistability predictions against variations in parameter values (supplementary figure S2 available at stacks.iop.org/PhysBio/7/036005/mmedia). Parameters were varied in pairs to determine the region of bistability. We observe that the most sensitive parameter is r_T, the dimensionless parameter representing total concentration of RseA, which regulates σ^E activity through inactive complex formation (cf equation (34)). This parameter can be varied
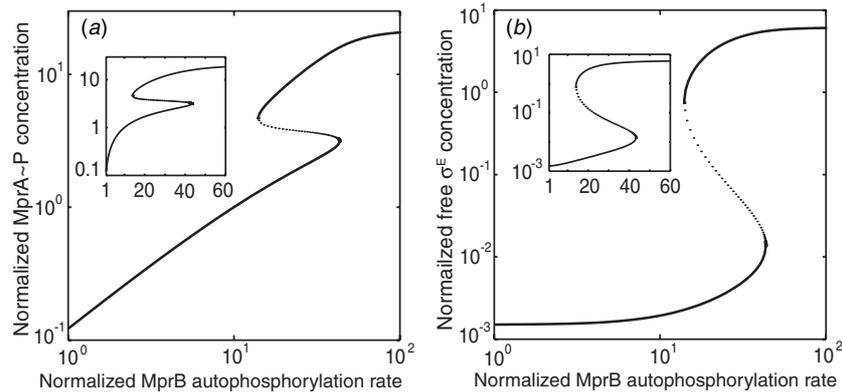
Figure 5. Bifurcation analysis in the complete mycobacterial stress-response network demonstrates bistability. (*a*), (*b*) Steady state concentrations of phosphorylated MprA (A_P) and of σ^E (E) versus MprB autophosphorylation rate (k_{ap}), the external signal representing the application of stress to the network. The two solid lines represent the stable steady states, which are separated by the unstable steady state (dotted line). Insets contain the respective bifurcation diagrams on a linear scale (X axis).

7-fold, while β_2^* and f_1, the dimensionless parameters representing basal transcription of MprA/MprB TCS from an σ^E-regulated promoter and amplification gain for an MprA~P regulated promoter (cf equation (33)), can be varied 50-fold without disturbing the bistability. The rest of the parameters can be varied at least 100-fold without affecting bistability. Thus, the mycobacterial stress-response network exhibits robust bistable behavior over a significant range of parameters.

2.6. Stochastic simulations reproduce bimodality in reporter gene expression

A flow cytometry study of *relA* transcription dynamics in *M. smegmatis* cells revealed bimodal distribution of gene expression in the population [20]. The observed distributions were time dependent so that the population with a low level of expression decreased and the high-expressing population grew with longer exposure to stress. To check if the observed bistability in a deterministic model will lead to a bimodal distribution of *relA* reporter as was observed in [20], we build a stochastic model for the MprAB/σ^E/RseA mycobacterial stress-response network. We expect that stochastic fluctuations in the elementary biochemical processes involving small numbers of reactant molecules can cause phenotypic switching between two physiological states [36]. To reproduce this result, we run stochastic simulations for our complete model comprising the MprA/MprB TCS and σ^E–RseA circuit along with a reporter gene under the control of σ^E (supplementary information available at stacks.iop.org/PhysBio/7/036005/mmedia). We run 10 000 simulation trajectories for 50 h (maximum duration of incubation in [20]) using the built-in stochastic simulator of COPASI [37].

We find that simulations produce bimodal distribution of reporter gene expression, with peaks corresponding to near basal and fully induced levels of *relA* reporter (figure 6). Furthermore, we observe that the number of cells showing induced expression slowly increases over time. These simulations correctly reproduce the qualitative behavior of
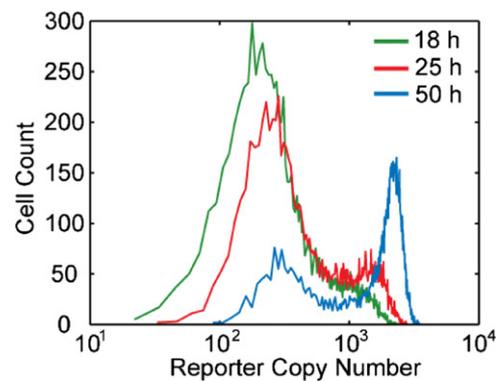
Figure 6. Bistability in the stress-response network results in bimodal distribution of reporter gene expression. Stochastic simulations of the MprA/MprB/σ^E network with 10 000 independent trajectories show bimodal reporter protein distribution. The heights of the two peaks (corresponding to basal and fully induced levels of the reporter gene) change with time (i.e. after 18, 25 and 50 h). The resulting distribution dynamics qualitatively agree with experimental data (cf figure 2 in [20]).

relA reporter expression in the population [20]. We do not expect this simplified model to quantitatively match experimental results, as it does not account for transcriptional bursting [38] or extrinsic noise sources [39]. Moreover, we have completely ignored the population dynamic aspects of the problem, i.e. assumed that cells grow with the same rate regardless of network dynamics. Nevertheless, the stochastic formulation of our deterministic model confirms that the bistability in the stress-response network is capable of producing the experimentally observed bimodal distribution of reporter gene expression.

3. Discussion

In this work we study the dynamical properties of the biochemical network possibly responsible for the persistence switch in mycobacteria. This switch plays a pivotal role in the spread of tuberculosis in host organisms, as persistent bacteria exhibiting reduced growth rates can survive drug treatment by

entering a latent state [5]. Recently, mycobacterial persistence has been linked to genes downstream of the stress-response network consisting of the MprA/MprB TCS, alternative sigma factor σ^E and its anti-sigma factor RseA [8, 9, 16]. This network contains two positive feedback loops. The first positive feedback loop originates through the positive autoregulation of the *mprAB* operon by the phosphorylated response regulator MprA~P [18]. The second positive feedback loop arises through the transcriptional regulation of *sigE* operon by MprA~P [19] and subsequent regulation of *mprAB* operon by σ^E [11]. We hypothesize that the various feedback loops operating in the network may lead to bistable behavior, thereby giving rise to population heterogeneity associated with persistence. Indeed, a recent experimental study of single-cell transcriptional reporters expressed from the *relA* promoter controlled by this network in *M. smegmatis* revealed bimodal distribution in the cell population [20].

We found that the first feedback loop, in the MprA/MprB TCS, is not sufficient to produce a bistable response in the physiologically relevant parameter range. The second feedback loop involving σ^E makes the network bistable, but only because of an increase in the effective cooperativity of the system arising from the post-translational regulation of σ^E by RseA. Thus, the network displays bistability that is robust to variation in parameter values. Essentially, the σ^E–RseA interaction follows the widespread mechanism of protein sequestration by an inhibitor which is known to exhibit an ultrasensitive response [33–35]. Furthermore, the stochastic formulation of our deterministic model qualitatively reproduces the experimentally observed bimodal distribution of reporter gene expression.

Our results have some general implications for the existence of bistability in core bacterial genetic networks with feedbacks. Our system contains representatives from two major classes of master-level transcriptional regulation modules in bacteria: a TCS [25] and an alternative σ/anti-σ factor network [40, 41]. Both these classes of networks often contain positive feedback loops, for example the PhoP/PhoQ, PhoB/PhoR and VanR/VanS TCSs [25] and the σ^F/UsfX [31], σ^R/RsrA [31] and σ^B/RsbW [42] σ/anti-σ systems that are sometimes hypothesized to be associated with bistability. Bistability has been demonstrated in the DegS/DegU TCS in *B. subtilis* which is of slightly different design as only DegU, the response regulator, is autoregulated [23]. The modular analysis we employed is capable of assessing implications of feedback regulation in each of these networks.

In many TCSs, genes for the response regulator and the sensory kinases are transcribed from the same operon, which is transcriptionally upregulated by the phosphorylated response regulator [25]. Our recent work on TCSs analyzes the physiological roles of this autoregulation and suggests that positive autoregulation does not necessarily give rise to an overall positive feedback [43]. The presence of a bifunctional sensory kinase in the autoregulated operon may result in a decrease of the phosphorylated fraction of the response regulator due to an increase in the phosphatase activity. The model predicts that some TCSs are capable of switching between positive and negative feedbacks depending on the biochemical characteristics. The ability to shift feedback signs allows the system to respond appropriately under different circumstances. Here we extend this analysis by analyzing whether this feedback can lead to bistability. We observe that the standard TCS with a bifunctional signaling histidine kinase is incapable of inducing bistability, unless the amplification gain due to the positive autoregulation is very large ($f \gg 10$) or there exists an exogenous phosphatase that dominates the dephosphorylation flux (effectively eliminating bifunctionality of the sensory kinase). Thus, because of the lack of a sufficiently strong feedback, positive autoregulation may not lead to bistability in TCSs with a bifunctional signaling histidine kinase. The intuitive explanation for this is similar to that for the results reported in [43]—negative feedback due to upregulation of the bifunctional sensory kinase transcription compensates the positive feedback component and decreases the bistability range. This additional function of bifunctionality of the sensory kinase—protection from bistability—also works for the bistability originating from TCS biochemical interactions proposed in [44].

Many alternative sigma factors are transcribed from autoregulated operons, and usually their activity is postranslationally modulated by anti-sigma factors. We have previously studied *B. subtilis* stress-response networks exhibiting the partner-switching mechanism in which the anti-σ^B factor (RsbW) forms complexes with either the σ^B factor or the anti-anti-σ^B factor (RsbV) [42]. In this network we did not observe bistability despite positive autoregulation of the *sigB* operon. A significant difference between that network and the one considered in this paper, besides the presence of the anti-anti-σ factor, is the physical arrangement of genes encoding σ and anti-σ factors. In the *B. subtilis* network, the sigma and anti-sigma genes are part of the same operon [42], while in the mycobacterial stress-response network the genes are part of two separate operons [32]. These results suggest that the arrangement in which the σ and the anti-σ factor genes belong to different and differentially regulated operons facilitates bistability. This prediction may be experimentally verified by constructing a strain in which both *sigE* and *rseA* are expressed from the native *sigE* promoter, in which case we expect the bistability to be lost. When the genes are part of the same operon, a negative feedback arises because the anti-σ factor sequesters the σ factor away from RNA polymerase, and thereby attenuates autoregulation. This negative feedback interferes with the positive feedback, diminishing its effect and leading to loss of bistability.

The effect of the interplay of two positive feedbacks on network bistability has been extensively studied theoretically and experimentally [45, 46]. Our analysis indicates that when two feedbacks control two independent additive promoters, then the second feedback will induce bistability in the system only when bistability already exists in the presence of the first feedback. We observe that, in the case of two feedbacks, the total LG is always less than the greater of the two individual LGs, which reduces the chances of bistability according to the formulated necessary condition. The rationale for this difference is the additive transcription from two promoters (cf equation (S24) available

at stacks.iop.org/PhysBio/7/036005/mmedia) of the *mprAB* operon, resulting in 'OR gate' between MprA∼P and σ^{E} activated transcription (activation of either promoter will be sufficient for *mprAB* expression). However, if the interplay of feedback loops causes multiplicative transcription, resulting in 'AND gate,' the presence of the second feedback will extend the range of bistability. These conclusions are in agreement with the results from a recent study on coupling of feedbacks [46].

The method developed here allowed us to identify exact biochemical interactions that facilitate bistability in the studied network and to find the parameter range that supports it robustly. Angeli and collaborators developed methods to deduce bistability for networks of arbitrary complexity that do not contain negative feedback loops [46]. This method cannot be applied to our system because the presence of the bifunctional sensory histidine kinase in the autoregulated operon can result in a negative feedback. Hence, we developed a new method for analyzing the presence of bistability in signaling networks by decoupling it into transcriptional and post-translational interaction modules. This separation reduces the dimensionality of the dynamical system and enables an independent input–output analysis in the two modules as they depend on non-overlapping sets of parameters. We formulate a general necessary condition for bistability based on LGs of the two modules, which is used to examine the existence of multiple steady states. A similar condition based on graphical method was used to study functions that can be combined together to operate as a switch in two repressor systems [47]. The log-gains used in this paper to formulate the bistability condition are essentially exponents of the effective power-law system representation [27]. In this sense, our method extends previous analysis of Savageau [27], who formulated a condition of bistability for some simple networks in terms of the reaction kinetic orders.

In the current model, we assumed constant degradation/dilution rates for all proteins. However, slow growth caused by σ^{E} overexpression could result in the dependence of growth rate on σ^{E} concentration, effectively strengthening the σ^{E}-dependent positive feedback in this system. Bistability due to growth retardation has been described recently [48] and will be included in future versions of this model. Also, we did not consider proteolytic degradation of RseA, which causes release of σ^{E} in conditions of surface stress and is associated with an additional feedback loop [17].

Despite these limitations, our model makes important biological predictions. We use the decoupling method to investigate the presence of bistability in the mycobacterial stress-response network, which was previously analyzed in [20]. We re-interpret their results within the framework of a comprehensive mathematical model based on the decoupling approximation. We show that the autoregulated MprA/MprB TCS cannot produce a bistable response and that σ^{E} post-translational regulation by the anti-sigma factor RseA is the key architectural feature that induces bistability in the system. Thus, only when the multiple positive feedbacks are combined with the ultrasensitive response of the σ^{E}–RseA interaction is bistability introduced in the system. Furthermore, in accord

with earlier research [33], we notice that the threshold and the degree of ultrasensitivity (measured using the LG of the interaction module in the σ^{E}–RseA circuit) depend on the total concentration of RseA. Evidently RseA plays an important role in the network, and we predict that its overexpression or deletion can eliminate bistability.

4. Methods

4.1. Decoupling approximation

The mycobacterial stress-response network was separated into transcriptional regulation and post-translational interaction modules based on the decoupling approximation. The mass-action equations and subsequent approximations are described in detail in supplementary information (cf equations (S20)–(S44) available at stacks.iop.org/PhysBio/7/036005/mmedia), while here only the equations corresponding to the decoupling approximation are considered.

The total concentrations of network proteins change slowly because of the different time scales of the two modules. The total concentrations of MprA (A_T), MprB (B_T) and σ^{E} (E_T) are defined as follows:

$$A_T = A + A_P + (A_P\text{-}B) + (A\text{-}B_P) \tag{21}$$

$$B_T = B + B_P + (A_P\text{-}B) + (A\text{-}B_P) \tag{22}$$

$$E_T = E + (E\text{-}R), \tag{23}$$

where A_P(B_P) and A(B) are the phosphorylated and unphosphorylated concentrations of MprA (MprB), respectively; E is free σ^{E} concentration; and A_P-B, A-B_P and E-R are the concentrations of complexes. Subsequently, the equations for the transcriptional regulation module were obtained by separating and adding together the individual protein production and degradation terms from equations (S30) and (S39)–(S43) available at stacks.iop.org/PhysBio/7/036005/mmedia:

$$\frac{\mathrm{d}A_T}{\mathrm{d}t} = \beta_1 \frac{\left(1 + f_1 \frac{A_P^2}{K_1}\right)}{\left(1 + \frac{A_P^2}{K_1}\right)} + \beta_2 \frac{\left(1 + f_2 \frac{E}{K_2}\right)}{\left(1 + \frac{E}{K_2}\right)} - k_{\mathrm{pdeg}} A_T \tag{24}$$

$$\frac{dB_T}{dt} = \lambda\beta_1 \frac{\left(1 + f_1 \frac{A_P^2}{K_1}\right)}{\left(1 + \frac{A_P^2}{K_1}\right)} + \lambda\beta_2 \frac{\left(1 + f_2 \frac{E}{K_2}\right)}{\left(1 + \frac{E}{K_2}\right)} - k_{\mathrm{pdeg}} B_T \tag{25}$$

$$\frac{\mathrm{d}E_T}{\mathrm{d}t} = \beta_3 \frac{\left(1 + f_3 \frac{A_P^2}{K_1}\right)}{\left(1 + \frac{A_P^2}{K_1}\right)} - k_{\mathrm{pdeg}} E_T, \tag{26}$$

where β_1, β_2, β_3 and f_1, f_2, f_3 are the basal transcription rates and amplification gains associated with promoters P_{AB}^1, P_{AB}^2, P_E, respectively; K_1 and K_2 are the equilibrium dissociation constants for MprA∼P–DNA and σ^{E}–DNA binding; and k_{pdeg} is the protein degradation rate. Comparing (24) and (25), we concluded that given zero or proportional initial conditions, the total concentrations of MprB and MprA stay proportional:

$$B_T = \lambda A_T \tag{27}$$

thereby reducing the dimensionality of the dynamical system. Therefore, from here onward the equation for B_T will not be considered and instead (27) will be used.

Gathering the phosphorylation terms from equations (S39)–(S42) and applying the quasi-steady state approximation, we are left with a set of linearly dependent equations. Two of these equations were substituted with the MprA and MprB conservation equations ((21) and (22)) to obtain

$$k_t \left(\frac{AB_P}{K_T} \right) - k_p \left(\frac{A_P B}{K_P} \right) + k_{\exp} A - k_{\text{exd}} A_P = 0 \quad (28)$$

$$k_{\text{ap}} B - k_{\text{ad}} B_P - k_t \left(\frac{AB_P}{K_T} \right) = 0 \quad (29)$$

$$A_T - A - A_P - \left(\frac{AB_P}{K_T} \right) - \left(\frac{A_P B}{K_P} \right) = 0 \quad (30)$$

$$\lambda A_T - B - B_P - \left(\frac{AB_P}{K_T} \right) - \left(\frac{A_P B}{K_P} \right) = 0. \quad (31)$$

Here, $k_t \left(\frac{AB_P}{K_T} \right)$ and $k_p \left(\frac{A_P B}{K_P} \right)$ represent fluxes for MprB-mediated phosphorylation and dephosphorylation of MprA (k_t and k_p are catalytic rates and K_T and K_P are Michaelis–Menten constants for respective MprB-dependent phosphorylation and dephosphorylation of MprA); $k_{\exp} A$ and $k_{\text{exd}} A_P$ represent fluxes for exogenous phosphorylation and dephosphorylation of MprA and $k_{\text{ap}} B$ and $k_{\text{ad}} B_P$ represent MprB autophosphorylation and dephosphorylation fluxes. The expressions (in parentheses) for $A - B_P$ and $A_P - B$ in (30) and (31) are from equations (S31) and (S32) available at stacks.iop.org/PhysBio/7/036005/mmedia. Equations (28)–(31) represent the phosphorylation module of the MprA/MprB TCS and are used to solve for $G(A_T)$ in equation (2). This solution is cumbersome to obtain analytically, but can be approximately calculated for certain limiting cases shown below.

Eliminating R and $(E - R)$ by using equations (23), (S33) and (S44), we arrive at the following relationship, which describes the σ^E–RseA interaction module:

$$E = -\frac{1}{2} [R_T - E_T + K_D]$$
$$+ \frac{1}{2} [(R_T - E_T + K_D)^2 + 4K_D E_T]^{1/2}, \quad (32)$$

where K_D is the equilibrium dissociation constant for the σ^E–RseA complex and E_T and R_T are the total concentrations of σ^E and RseA, respectively. Equations (28)–(32) describe the post-translational interaction module.

To reduce the number of free parameters in the system A_T, the concentrations A_P, A, B_P and B were normalized by $\beta_1 / k_{\text{pdeg}}$, whereas E and E_T were normalized by $\beta_3 / k_{\text{pdeg}}$. This gave rise to the following dimensionless parameters apart from f_1, f_2, f_3 and λ:

$$k_t^* = \frac{k_t}{k_{\text{pdeg}}}, \quad k_p^* = \frac{k_p}{k_{\text{pdeg}}}, \quad k_{\text{ap}}^* = \frac{k_{\text{ap}}}{k_{\text{pdeg}}}, \quad k_{\text{ad}}^* = \frac{k_{\text{ad}}}{k_{\text{pdeg}}},$$
$$k_{\exp}^* = \frac{k_{\exp}}{k_{\text{pdeg}}}, \quad k_{\text{exd}}^* = \frac{k_{\text{exd}}}{k_{\text{pdeg}}}, \quad \beta_2^* = \frac{\beta_2}{\beta_1} \quad (33)$$

$$K_T^* = \frac{K_T k_{\text{pdeg}}}{\beta_1}, \quad K_P^* = \frac{K_P k_{\text{pdeg}}}{\beta_1}, \quad K_1^* = \frac{K_1 k_{\text{pdeg}}^2}{\beta_1^2},$$
$$K_2^* = \frac{K_2 k_{\text{pdeg}}}{\beta_3}, \quad K_D^* = \frac{K_D}{R_T}, \quad r_T = \frac{R_T k_{\text{pdeg}}}{\beta_3}. \quad (34)$$

The normalized concentrations and dimensionless parameters were used in all the simulations.

4.2. Examining MprA/MprB TCS for bistability

The equation for the transcriptional regulation (autoregulation) module of the MprA/MprB TCS was obtained by substituting $\beta_2 = 0$ in (24) which results in (1), where

$$F(A_P) = \frac{\beta_1}{k_{\text{pdeg}}} \frac{\left(1 + f_1 \frac{A_P^2}{K_1} \right)}{\left(1 + \frac{A_P^2}{K_1} \right)}. \quad (35)$$

Equations (28)–(31) describe the post-translational interaction (phosphorylation) module. This set of equations reduces to (2) where G depicts the functional dependence of A_P on A_T.

The necessary condition based on the LGs of modules (equation (5)) was used to evaluate the MprA/MprB TCS for bistability. The LG for the autoregulation module (equation (6)) and its maximum value (equation (7)) were calculated analytically, whereas the LG for the phosphorylation module (equation (3)) and its maximum value were calculated numerically. The *fsolve* and *ga* optimization functions in MATLAB (R2009a, The Mathworks) were used to solve the system of equations and to compute the maximum value, respectively. In the absence of exogenous phosphorylation–dephosphorylation of MprA ($k_{\text{exd}} = k_{\exp} = 0$) and irreversible autophosphorylation of MprB ($k_{\text{ad}} = 0$), equations (28)–(31) were analytically solved to obtain the LG for the phosphorylation module:

$$\text{LG}_P = \begin{cases} 1, & A_T < \frac{K_P k_{\text{ap}}}{k_p} \\ 0, & A_T > \frac{K_P k_{\text{ap}}}{k_p} \end{cases}. \quad (36)$$

4.3. Examining the MprA/MprB/σ^E network for bistability

In this subnetwork, our analysis was restricted to the LG of the transcriptional regulation (autoregulation) module, because inclusion of the σ^E-mediated feedback affected only the transcriptional interactions in the MprA/MprB TCS studied above. In the absence of the anti-sigma factor RseA, σ^E–RseA complex is not formed and therefore $E_T = E$. The autoregulation module equations are the same as (24) and (26), the only difference being that E in (24) was replaced by E_T. These equations are equivalent to (8) and (9), where

$$F^D = \frac{\beta_1}{k_{\text{pdeg}}} \frac{\left(1 + f_1 \frac{A_P^2}{K_1} \right)}{\left(1 + \frac{A_P^2}{K_1} \right)}, \qquad F^I = \frac{\beta_2}{k_{\text{pdeg}}} \frac{\left(1 + f_2 \frac{E}{K_2} \right)}{\left(1 + \frac{E}{K_2} \right)} \quad \text{and}$$

$$H = \frac{\beta_3}{k_{\text{pdeg}}} \frac{\left(1 + f_3 \frac{A_P^2}{K_1} \right)}{\left(1 + \frac{A_P^2}{K_1} \right)}. \quad (37)$$

At the steady state, the expression for E_T was substituted from (9) into (8) to obtain the following equation, which is equivalent to (10):

$$F = \beta_1' \frac{\left(1 + f_1 \frac{A_P^2}{K_1}\right)}{\left(1 + \frac{A_P^2}{K_1}\right)} + \beta_{\text{eff}}' \frac{\left(1 + f_{\text{eff}} \frac{A_P^2}{K_{\text{eff}}}\right)}{\left(1 + \frac{A_P^2}{K_{\text{eff}}}\right)}, \quad (38)$$

where

$$\beta_i' = \frac{\beta_i}{k_{\text{pdeg}}} (i \in 1, 2, 3) \quad \text{and} \quad \beta_{\text{eff}}' = \beta_2' \frac{\left(1 + \frac{f_2 \beta_3'}{K_2}\right)}{\left(1 + \frac{\beta_3'}{K_2}\right)} \quad (39)$$

$$K_{\text{eff}} = K_1 \frac{\left(1 + \frac{\beta_3'}{K_2}\right)}{\left(1 + \frac{f_3 \beta_3'}{K_2}\right)} \quad \text{and} \quad f_{\text{eff}} = \frac{\left(1 + \frac{f_2 f_3 \beta_3'}{K_2}\right)\left(1 + \frac{\beta_3'}{K_2}\right)}{\left(1 + \frac{f_2 \beta_3'}{K_2}\right)\left(1 + \frac{f_3 \beta_3'}{K_2}\right)}, \quad (40)$$

where f_{eff} is the effective amplification gain due to the indirect feedback composed of the transcriptional regulation of the *sigE* operon by MprA~P and of the *mprAB* operon by σ^{E} and K_{eff} is the effective dissociation constant for MprA~P–DNA binding in the case of the indirect feedback.

In (38), the first and second terms represent the direct and indirect feedbacks to the *mprAB* operon, respectively. Since the two terms have the same functional form and differ only in the constants (β, f, K), the expressions for their maximum LGs are also similar (equations (7) and (13)). Furthermore, the maximum for LG_A^I (equation (13)) depends on f_{eff} (equation (40)). In order to calculate max $\left(\text{LG}_A^I\right)$, max($f_{\text{eff}}$) was obtained by finding the maxima of f_{eff} as a function of $\frac{\beta_3'}{K_2}$:

$$\max(f_{\text{eff}}) = \left(\frac{1 + \sqrt{f_2 f_3}}{\sqrt{f_2} + \sqrt{f_3}}\right)^2. \quad (41)$$

This equation gives rise to the inequalities max(f_{eff}) < f_2 and max(f_{eff}) < f_3 for $f_2 > 1$ and $f_3 > 1$, respectively, which were used to establish the inequality in (15). The total LG for the autoregulation module (equation (12)) was calculated from (38) using the relationship defined in (11) and was subsequently subjected to the necessary condition (equation (5)) to analyze the presence of bistability in the MprA/MprB/σ^{E} network.

4.4. Examining the σ^{E}–RseA network for bistability

To reduce analytical complexity, the MprA/MprB TCS (equations (24), (28)–(31)) was not explicitly considered in this subnetwork. Instead, σ^{E} autoregulation was included, which can be perceived as a combination of the transcriptional regulation of the *mprAB* operon by σ^{E} and of the *sigE* operon by MprA~P. The autoregulation module was modeled in (16), where

$$U(E) = \frac{\beta}{k_{\text{pdeg}}} \frac{\left(1 + f \frac{E^q}{K^q}\right)}{\left(1 + \frac{E^q}{K^q}\right)}, \quad (42)$$

where β and f are the basal transcription rate and the amplification gain associated with the autoregulated *sigE*

promoter; K is the σ^{E} concentration at which the transcription rate is half activated from its maximum value $\left(\sim \frac{\beta f}{2}\right)$ and q is the effective Hill coefficient.

The interaction module described earlier in (32) is equivalent to (17), where V describes the functional dependence of E on E_T. The LGs for the autoregulation and interaction modules were analytically calculated using (16) and (32), respectively, at the steady state:

$$\text{LG}_A = \frac{q \frac{E^q}{K^q} (f - 1)}{\left(1 + \frac{E^q}{K^q}\right)\left(1 + f \frac{E^q}{K^q}\right)} \quad (43)$$

$$\text{LG}_I = \frac{(E^2 + (2K_D + R_T) E + K_D (K_D + R_T))}{(E^2 + 2K_D E + K_D (K_D + R_T))}. \quad (44)$$

The maximum values of LG_A and LG_I ((18) and (19)) were computed analytically using (43) and (44). These were constrained by the necessary condition (equation (20)) to obtain a sample parameter set for which the σ^{E}–RseA network exhibits bistability (figure 4(*c*)).

4.5. Examining the complete mycobacterial stress-response network for bistability

The equations for the transcriptional regulation (autoregulation) and post-translational interaction modules for the complete network were described earlier (equations (S39)–(S43) and (32) with $k_{\text{exp}} = k_{\text{exd}} = 0$). The LG for the autoregulation module $\left(\text{LG}_A = \frac{E}{E_T} \frac{\partial E_T}{\partial E}\right)$ was computed numerically from equations (S39)–(S43) at the steady state. The *fsolve* function in MATLAB was used to solve the system of equations. The LG for the σ^{E}–RseA interaction module $\left(\text{LG}_I = \frac{E_T}{E} \frac{\partial E}{\partial E_T}\right)$ was computed using (44). These LGs were constrained by the necessary condition (20) to obtain a sample parameter set for which the complete mycobacterial stress-response network exhibits bistability (figure 4(*d*)).

References

[1] Lewis K 2007 Persister cells, dormancy and infectious disease *Nat. Rev. Microbiol.* **5** 48–56
[2] Kaern M, Elston T C, Blake W J and Collins J J 2005 Stochasticity in gene expression: from theories to phenotypes *Nat. Rev. Genet.* **6** 451–64

[3] Balaban N Q, Merrin J, Chait R, Kowalik L and Leibler S 2004 Bacterial persistence as a phenotypic switch *Science* **305** 1622–5

[4] Keren I, Shah D, Spoering A, Kaldalu N and Lewis K 2004 Specialized persister cells and the mechanism of multidrug tolerance in *Escherichia coli J. Bacteriol.* **186** 8172–80

[5] Stewart G R, Robertson B D and Young D B 2003 Tuberculosis: a problem with persistence *Nat. Rev. Microbiol.* **1** 97–105

[6] Parrish N M, Dick J D and Bishai W R 1998 Mechanisms of latency in *Mycobacterium tuberculosis Trends Microbiol.* **6** 107–12

[7] Balázsi G, Heath A P, Shi L and Gennaro M L 2008 The temporal response of the *Mycobacterium tuberculosis* gene regulatory network during growth arrest *Mol. Syst. Biol.* **4** 225

[8] Zahrt T C and Deretic V 2001 *Mycobacterium tuberculosis* signal transduction system required for persistent infections *Proc. Natl Acad. Sci. USA* **98** 12706–11

[9] Manganelli R, Dubnau E, Tyagi S, Kramer F R and Smith I 1999 Differential expression of 10 sigma factor genes in *Mycobacterium tuberculosis Mol. Microbiol.* **31** 715–24

[10] Betts J C, Lukey P T, Robb L C, McAdam R A and Duncan K 2002 Evaluation of a nutrient starvation model of *Mycobacterium tuberculosis* persistence by gene and protein expression profiling *Mol. Microbiol.* **43** 717–31

[11] Manganelli R, Voskuil M I, Schoolnik G K and Smith I 2001 The *Mycobacterium tuberculosis* ECF sigma factor sigmaE: role in global gene expression and survival in macrophages *Mol. Microbiol.* **41** 423–37

[12] Berney M and Cook G M 2010 Unique flexibility in energy metabolism allows mycobacteria to combat starvation and hypoxia *PLoS One* **5** e8614

[13] Dahl J L, Kraus C N, Boshoff H I, Doan B, Foley K, Avarbock D, Kaplan G, Mizrahi V, Rubin H and Barry C E III 2003 The role of RelMtb-mediated adaptation to stationary phase in long-term persistence of *Mycobacterium tuberculosis* in mice *Proc. Natl Acad. Sci. USA* **100** 10026–31

[14] Zahrt T C, Wozniak C, Jones D and Trevett A 2003 Functional analysis of the *Mycobacterium tuberculosis* MprAB two-component signal transduction system *Infect. Immun.* **71** 6962–70

[15] Sureka K, Dey S, Datta P, Singh A K, Dasgupta A, Rodrigue S, Basu J and Kundu M 2007 Polyphosphate kinase is involved in stress-induced mprAB-sigE-rel signalling in mycobacteria *Mol. Microbiol.* **65** 261–76

[16] Dona V, Rodrigue S, Dainese E, Palu G, Gaudreau L, Manganelli R and Provvedi R 2008 Evidence of complex transcriptional, translational, and posttranslational regulation of the extracytoplasmic function sigma factor sigmaE in *Mycobacterium tuberculosis J. Bacteriol.* **190** 5963–71

[17] Barik S, Sureka K, Mukherjee P, Basu J and Kundu M 2009 RseA, the SigE specific anti-sigma factor of *Mycobacterium tuberculosis*, is inactivated by phosphorylation-dependent ClpC1P2 proteolysis *Mol. Microbiol.* **75** 592–606

[18] He H and Zahrt T C 2005 Identification and characterization of a regulatory sequence recognized by *Mycobacterium tuberculosis* persistence regulator MprA *J. Bacteriol.* **187** 202–12

[19] He H, Hovey R, Kane J, Singh V and Zahrt T C 2006 MprAB is a stress-responsive two-component system that directly regulates expression of sigma factors SigB and SigE in *Mycobacterium tuberculosis J. Bacteriol.* **188** 2134–43

[20] Sureka K, Ghosh B, Dasgupta A, Basu J, Kundu M and Bose I 2008 Positive feedback and noise activate the stringent response regulator rel in mycobacteria *PLoS One* **3** e1771

[21] Shinar G, Milo R, Martinez M R and Alon U 2007 Input output robustness in simple bacterial signaling systems *Proc. Natl Acad. Sci. USA* **104** 19931–5

[22] Kierzek A M, Zhou L and Wanner B L 2010 Stochastic kinetic model of two component system signalling reveals all-or-none, graded and mixed mode stochastic switching responses *Mol. Biosyst.* **6** 531–42

[23] Veening J W, Igoshin O A, Eijlander R T, Nijland R, Hamoen L W and Kuipers O P 2008 Transient heterogeneity in extracellular protease production by Bacillus subtilis *Mol. Syst. Biol.* **4** 184

[24] Ferrell J E Jr 2002 Self-perpetuating states in signal transduction: positive feedback, double-negative feedback and bistability *Curr. Opin. Cell. Biol.* **14** 140–8

[25] Mitrophanov A Y and Groisman E A 2008 Positive feedback in cellular control systems *Bioessays* **30** 542–55

[26] Alon U 2007 *An Introduction to Systems Biology: Design Principles of Biological Circuits* (Boca Raton, FL: Chapman and Hall)

[27] Savageau M A 2002 Alternative designs for a genetic switch: analysis of switching times using the piecewise power-law representation *Math. Biosci.* **180** 237–53

[28] Miyashiro T and Goulian M 2008 High stimulus unmasks positive feedback in an autoregulated bacterial signaling circuit *Proc. Natl Acad. Sci. USA* **105** 17457–62

[29] Batchelor E and Goulian M 2003 Robustness and the cycle of phosphorylation and dephosphorylation in a two-component regulatory system *Proc. Natl Acad. Sci. USA* **100** 691–6

[30] Pang X, Vu P, Byrd T F, Ghanny S, Soteropoulos P, Mukamolova G V, Wu S, Samten B and Howard S T 2007 Evidence for complex interactions of stress-associated regulons in an mprAB deletion mutant of *Mycobacterium tuberculosis Microbiology* **153** 1229–42

[31] Manganelli R, Provvedi R, Rodrigue S, Beaucher J, Gaudreau L and Smith I 2004 Sigma factors and global gene regulation in *Mycobacterium tuberculosis J. Bacteriol.* **186** 895–902

[32] White M J, He H, Penoske R M, Twining S S and Zahrt T C 2010 PepD participates in the mycobacterial stress response mediated through MprAB and SigE *J. Bacteriol.* **192** 1498–510

[33] Buchler N E and Cross F R 2009 Protein sequestration generates a flexible ultrasensitive response in a genetic network *Mol. Syst. Biol.* **5** 272

[34] Ferrell J E Jr 1996 Tripping the switch fantastic: how a protein kinase cascade can convert graded inputs into switch-like outputs *Trends Biochem. Sci.* **21** 460–6

[35] Lenz D H, Mok K C, Lilley B N, Kulkarni R V, Wingreen N S and Bassler B L 2004 The small RNA chaperone Hfq and multiple small RNAs control quorum sensing in Vibrio harveyi and *Vibrio cholerae Cell* **118** 69–82

[36] Choi P J, Cai L, Frieda K and Xie X S 2008 A stochastic single-molecule event triggers phenotype switching of a bacterial cell *Science* **322** 442–6

[37] Hoops S, Sahle S, Gauges R, Lee C, Pahle J, Simus N, Singhal M, Xu L, Mendes P and Kummer U 2006 COPASI–a complex pathway simulator *Bioinformatics* **22** 3067–74

[38] Golding I, Paulsson J, Zawilski S M and Cox E C 2005 Real-time kinetics of gene activity in individual bacteria *Cell* **123** 1025–36

[39] Elowitz M B, Levine A J, Siggia E D and Swain P S 2002 Stochastic gene expression in a single cell *Science* **297** 1183–6

[40] Wosten M M 1998 Eubacterial sigma-factors *FEMS Microbiol. Rev.* **22** 127–50

[41] Hughes K T and Mathee K 1998 The anti-sigma factors *Annu. Rev. Microbiol.* **52** 231–86

[42] Igoshin O A, Brody M S, Price C W and Savageau M A 2007 Distinctive topologies of partner-switching signaling networks correlate with their physiological roles *J. Mol. Biol.* **369** 1333–52

[43] Ray J C and Igoshin O A 2010 Adaptable functionality of transcriptional feedback in bacterial two-component systems *PLoS Comput. Biol.* **6** e1000676

[44] Igoshin O A, Alves R and Savageau M 2008 Hysteretic and graded responses in bacterial two-component signal transduction *Mol. Microbiol.* **68** 1196–215

[45] Brandman O, Ferrell J E Jr, Li R and Meyer T 2005 Interlinked fast and slow positive feedback loops drive reliable cell decisions *Science* **310** 496–8

[46] Chang D E, Leung S, Atkinson M R, Reifler A, Forger D and Ninfa A J 2009 Building biological memory by linking positive feedback loops *Proc. Natl Acad. Sci. USA* **107** 175–80

[47] Cherry J L and Adler F R 2000 How to make a biological switch *J. Theor. Biol.* **203** 117–33

[48] Tan C, Marguet P and You L 2009 Emergent bistability by a growth-modulating positive feedback circuit *Nat. Chem. Biol.* **5** 842–8